16th World Congress in Computational Mechanics (WCCM)
21-26 July 2024, Vancouver, Canada
A. Korobenko, M. Laforet, S. Prudhomme, R. Vaziri (Eds)

PROJECTOR ASSEMBLY: BRIDGING POISSON AND ELASTICITY FORMULATIONS

TIAGO F. MOHERDAUI[1], ALFREDO G. NETO[2] AND PETER WRIGGERS[3]

[1] Universidade de São Paulo
Av. Prof. Almeida Prado, 83, 05508-070, São Paulo, Brazil
tiago.moherdaui@usp.br

[2] Universidade de São Paulo
Av. Prof. Almeida Prado, 83, 05508-070, São Paulo, Brazil
alfredo.gay@usp.br

[3] Leibniz Universität Hannover
An der Universität 1, building 8142, 30823 Garbsen, Germany
wriggers@ikm.uni-hannover.de

Key words: VEM, Poisson Problem, Elasticity Problems.

Abstract. Virtual element methods define their shape functions implicitly (tailored to each element's geometry), foregoing the typical reference element and transformation scheme usually employed by the finite element method. The formulation leverages the use of polynomial projections supplied by heuristic stabilizations when necessary. These projections are represented by projector matrices, which require the solution of a local system. Elasticity formulations usually employ an L^2-projection from a displacement multifield onto a strain multifield, requiring the solution of a considerably larger system than a typical Poisson problem would require, with dense matrices and lots of zeroes. This work presents a way to obtain the projections for elasticity formulation by assembling from the L^2-projection for each derivative of the one-field a Poisson formulation, resulting in smaller local systems being solved and more efficient storage. This approach is based on the linearity of both projections and derivatives, and is shown in the examples to preserve the convergence rate of the method.

1 INTRODUCTION

The virtual element method (VEM) has seen significant advances since its introduction in [1]. These pertain both to formulations of the method (see, e.g., [2, 3, 4, 5, 6]), and to many different applications, such as: topology optimization [7, 8], multiscale modelling [9] and homogenization [10, 11, 12], flexible particle modeling [13] and contact [14, 15], to mention a few examples.

The method consists in a generalization of the Finite Element Method (FEM) to polytope element domains. This is achieved by introducing an implicitly defined function space that guarantees, by design, the desired convergence properties (i.e., a full polynomial subspace). The degrees of freedom are such that a polynomial projector onto said subspace is computable

without additional information. The remaining construction of the method is based on the use of the polynomial projection of the functions of the space to compute the discrete terms (stiffness matrix and righthand-side) with the eventual supplementation with a stabilization term. Computability of the relevant projections is a core feature of any virtual element formulation, and their practical computation is also of importance in concrete implementations.

This work presents a brief overview on two formulations of conformal virtual elements for Poisson's equations in two dimensions and how they translate into equivalent formulations for plane linear elasticity by using the assembly of the projection operators. This is useful as the formulation is simpler to compute, easier to test and debug, also incurring smaller local linear systems to be solved for the projectors.

The outline of the work is as follows. The underlying problem formulations are presented in Section 2. The different virtual element formulations employed are presented in Section 3. The projector assembly concept is presented in Section 4. Numerical examples are provided in Section 5.

2 PROBLEM FORMULATION

Two different partial differential equations are discussed in this work. The first are Poisson's equations, as they provide the simpler framework in which to compute the projectors. The second is that of plane linear elasticity, here represented by the plane strain case, representing the target framework for their use.

2.1 Poisson's Equations in 2D

The problem consists in finding the solution (u), whose Laplacian inside a domain ($\Omega \subset \mathbb{R}^2$) is prescribed as $-f$. The boundary is partitioned into Dirichlet (Γ_D) and Neumann (Γ_N) boundary condition domains, with $\boldsymbol{n}$ being the external unit normal vector at the latter. The differential formulation is presented in (1).

$$\begin{cases} \Delta u(\boldsymbol{x}) = -f(\boldsymbol{x}), \forall \boldsymbol{x} \in \Omega; \\ u(\boldsymbol{x}) = \bar{u}(\boldsymbol{x}), \forall \boldsymbol{x} \in \Gamma_D; \\ \nabla u(\boldsymbol{x}) \cdot \boldsymbol{n}(\boldsymbol{x}) = g(\boldsymbol{x}), \forall \boldsymbol{x} \in \Gamma_N. \end{cases} \tag{1}$$

The weak formulation of the problem is presented below, where $H_D^1(\Omega)$ and $H_0^1(\Omega)$ are, respectively, the space of the functions in $H^1(\Omega)$ that satisfy the Dirichlet boundary conditions, and those which assume null value in Γ_D.

Find $u \in H_D^1(\Omega)$ s.t. $\forall\, \delta u \in H_0^1(\Omega)$:

$$\int_\Omega (\nabla u \cdot \nabla \delta u) d\boldsymbol{x} = \int_\Omega f \delta u d\boldsymbol{x} + \int_{\Gamma_N} g \delta u d\sigma. \tag{2}$$

2.2 Plane Strain Linear Elasticity

The formulation for this problem is introduced using Voigt notation. In this case, the solution comprises the displacement field ($\boldsymbol{u} \in \mathbb{R}^2$) whose strains ($\boldsymbol{\varepsilon}(\boldsymbol{u}) = \boldsymbol{S}\boldsymbol{u}$, with $\boldsymbol{S} = \begin{bmatrix} \partial_x & 0 & \partial_y \\ 0 & \partial_y & \partial_x \end{bmatrix}^T$), and associated stresses through Hooke's law ($\boldsymbol{\sigma} = \boldsymbol{C}\boldsymbol{\varepsilon}$) satisfy the balance

equations considering volume load $\boldsymbol{b}$, surface load $\boldsymbol{t}$ as Neumann boundary conditions, and prescribed displacements $\overline{\boldsymbol{u}}$ as Dirichlet boundary conditions. Balance is here represented by the weak formulation in (3), with similar definitions for $\Omega, \Gamma_{\mathrm{D}}, \Gamma_N, H_D^1$ and H_0^1.

Find $\boldsymbol{u} \in [H_D^1(\Omega)]^2$ s.t. $\forall\ \boldsymbol{\delta u} \in [H_0^1(\Omega)]^2$:

$$\int_\Omega \boldsymbol{\varepsilon}(\boldsymbol{\delta u}) \cdot \boldsymbol{\sigma}(\boldsymbol{u}) d\boldsymbol{x} = \int_\Omega (\boldsymbol{\delta u} \cdot \boldsymbol{b}) d\boldsymbol{x} + \int_{\Gamma_N} (\boldsymbol{\delta u} \cdot \boldsymbol{t}) d\sigma. \tag{3}$$

3 VIRTUAL ELEMENT FORMULATIONS

The method has many different formulations. In this section we focus on presenting a brief overview of two of them: the serendipity formulation with [3] and without stabilization [16]. For simplicity, these formulations are presented for two dimensions, however they have three-dimensional counterparts [17, 18] and the projector assembly works for both cases. The formulation introduction will be very brief, the authors recommend reading their original works for more detailed information.

Let the domain Ω be partitioned into a collection $\mathcal{T}_h$ of polygonal elements. A generic element $E \in \mathcal{T}_h$ has n_V vertices and edges, area $|E|$, and diameter h_E. For each element, let there be a local function space, for now denoted $V_k(E)$, with the space of polynomials up to order k, here denoted $P_k(E)$, as a subspace.

The auxiliar space, $\mathcal{B}_k$, defined over the boundary of the element, is as follows

$$\mathcal{B}_k(\partial E) \coloneqq \{v \in C^0(\partial E) \mid v \in P_k(e), \forall e \in \partial E\}, \tag{4}$$

where $P_k(\mathrm{D} \subset \mathbb{R}^d)$, is the space of polynomials of order up to k in d variables over V, and e denotes a generic edge in ∂E.

3.1 Serendipity VEM Space

The serendipity VEM space, $V_k^S(E)$, introduced in [3] is defined as

$$\begin{aligned} &\tilde{V}_k^S(E) \coloneqq \{v \in H^1(E) \cap \mathcal{B}_k(\partial E) | \Delta v \in P_k(E)\}, \\ &V_k^S(E) \coloneqq \left\{v \in \tilde{V}_k^S(E) \middle| \int_E vp d\boldsymbol{x} = \int_E \Pi_k^S vp d\boldsymbol{x}, \forall p \in \left(P_k / P_{k-\eta_E}\right)(E)\right\}. \end{aligned} \tag{5}$$

An auxiliar space $\tilde{V}_k^S$ is introduced, and the actual space is defined as the analog of a level set where the polynomial moments of these functions with respect to certain polynomial orders coincide with those of the serendipity projection Π_k^S. The orthogonality condition for this projector is based on the Euclidean inner product of the degree of freedom vector. Furthermore, moments are supplied by this projection in substitution to internal degrees of freedom if $\eta_E > 2$, where η_E is the number of support lines that define ∂E. For linear and quadratic elements, this implies no internal degrees of freedom are necessary in 2D, thus only the boundary degrees of freedom (values at vertices and $k-1$ points at edges) are left.

For the discrete weak formulation, both the original Π_k^∇ and the L^2 projection of the gradient of the solution ($\Pi_{k-1}^0 \nabla$) are computable. That is, one can use either $\nabla \Pi_k^\nabla u_h$ or $\Pi_{k-1}^0 \nabla u_h$ as projections of the gradient of trial and test functions in (2). The choice for this work is to use the latter, as it is shown to be more robust for higher order elements [19].

3.2 Serendipity Enlarged Enhanced VEM Space

The serendipity self-stabilized VEM space $V_{k,l}^{SF}(E)$, known in the literature as Serendipity Enlarged Enhanced VEM space, is based on the recent approach for self-stabilized virtual elements through projection of the gradient (or other differential operator) of the solution into a higher order polynomial space. This supplies the missing rank in the stiffness matrix. This was originally proposed in [20], developed along the serendipity formulation in [16], and being further expanded in [18, 21]. In this work the formulation in [16] is presented.

$$\begin{aligned} &\tilde{V}_{k,l}^{SF}(E) \coloneqq \{v \in H^1(E) \cap \mathcal{B}_k(\partial E) | \Delta v \in P_{l-1}(E)\}, \\ &V_{k,l}^{SF}(E) \coloneqq \left\{v \in \tilde{V}_{k,l}^{SF}(E) \middle| \int_E vpd\boldsymbol{x} = \int_E \Pi_k^S vpd\boldsymbol{x}, \forall p \in \left(P_{l-1}/P_{k-\eta_E}\right)(E)\right\}. \end{aligned} \tag{6}$$

This formulation relies on the computation of the L^2 projection of the gradient of a function ($\Pi_l^0 \nabla u_h$) into the space $(P_l)^d$, usually with $l > k-1$, chosen so as to stabilize the element. The computability of this projection requires additional internal degrees of freedom, i.e., those associated with monomials up to order $l-1$, however, the serendipity formulation supplies these moments up to a certain order, as described earlier. Both parameters, l and η_E, depend on the geometry of the element. They define the actual number of internal degrees of freedom required for the element. However, the usual case for orders $k = 1$ and 2 for Voronoi meshes lead to no internal degrees of freedom remaining for the self-stabilized elements.

4 PROJECTOR ASSEMBLY

This section presents the core concept of the work. It shows how some basic projectors can be used to construct more complex ones, with the main example being the projector of the linear strains. This is followed by a subsection with some considerations on how this can be more efficient than direct computation.

The projectors required for full implementation of the elements are Π_k^S, Π_k^0 and $\Pi_l^0 \nabla$ (with $l = k-1$ for the formulation that requires stabilization), in the case of Poisson elements. For the elasticity case, $\boldsymbol{\Pi_k^S}$, $\boldsymbol{\Pi_k^0}$ and $\boldsymbol{\Pi_l^0 \varepsilon}$, here in bold to represent the vectorial nature of the argument of the projection.

The assembly process for the serendipity and L^2 projection of the solution is very direct. For example, if one assumes $\boldsymbol{u_h} \in (V_k)^2 = \{u_0 \quad u_1\}^T$ and n_{DOF} being the number of degrees of freedom of V_h, then $\boldsymbol{\Pi_k^0}$ and Π_k^0 have $(2n_k \times 2n_{DOF})$ and $(n_k \times n_{DOF})$ matrix representations, respectively, with $n_k = \dim P_k(E)$. The representations are such that the following holds

$$\boldsymbol{\Pi_k^0 u_h} = \{\Pi_k^0 u_0 \quad \Pi_k^0 u_1\}^T. \tag{7}$$

the same holding with $\boldsymbol{\Pi_k^S}$ and Π_k^S.

The relation between $\Pi_l^0 \nabla$ and $\boldsymbol{\Pi_l^0 \varepsilon}$ requires intermediary steps. First, one decomposes $\Pi_l^0 \nabla : V_k \to (P_l)^d$ into its partial derivative components, i.e., $\Pi_l^0 \partial_{x_j} : V_k \to P_l$, such that

$$\Pi_l^0 \nabla u_h = \left\{\Pi_l^0 \partial_{x_0} u_h \quad \Pi_l^0 \partial_{x_1} u_h\right\}^T. \tag{8}$$

Considering that the typical procedure of computing the matrix representation of a projector can be summarized as follows, using the notation in [22]

$$\boldsymbol{\Pi} = \boldsymbol{G^{-1} B}, \tag{9}$$

where $\boldsymbol{G}$ involves integrals of monomials and $\boldsymbol{B}$ the monomial moments of the basis functions ϕ_i of V_k. For example, for Π_k^0, $G_{\alpha\beta} = \int_E m_\alpha m_\beta d\boldsymbol{x}$ and $B_{\alpha i} = \int_E \phi_i m_\alpha d\boldsymbol{x}$. The computations in B usually involve some use of integration by parts or the divergence theorem to put the integrals in terms of the degrees of freedom of the virtual element space.

Due to the linearity of projections and derivatives, one can assemble the projector of the strains from the projectors of partial derivatives

$$\boldsymbol{\Pi_l^0 \varepsilon}(\boldsymbol{u_h}) = \left\{\Pi_l^0 \partial_{x_0} u_0 \quad \Pi_l^0 \partial_{x_1} u_1 \quad \Pi_l^0 \partial_{x_1} u_0 + \Pi_l^0 \partial_{x_0} u_1\right\}^T \tag{10}$$

4.1 Considerations

The definition of every projector, especially if no constitutive quantity is involved, depends exclusively on the geometry of the element. Therefore, the problem in (10) must be solved for each required projector for each element in the mesh. This task can be frontloaded, being computed at the start of solution procedure, and the projectors stored in memory. The use of projector assembly helps reduce the size of the system that must be solved for each projector, improves reusability of partial results, while allowing the construction of more complex projectors.

As a first example, consider the computation of $\Pi_l^0 \nabla$, in the context of Poisson's equations. Usually, the computation of the projector in (9) is split into two steps: a decomposition of $\boldsymbol{G}$, and a solution step for $\boldsymbol{B}$, resulting in $\boldsymbol{\Pi}$. The typical direct procedure would require the decomposition of a $(2n_l \times 2n_l)$ matrix $\boldsymbol{G}$, and solution for a $(2n_l \times n_{DOF})$ matrix $\boldsymbol{B}$. If one were to split into the two partial derivatives, this would lead to the same matrix $\boldsymbol{G}$ of size $(n_l \times n_l)$ being decomposed and used in the solution step for two matrices $\boldsymbol{B}$ $(n_l \times n_{DOF})$, one for each derivative. Therefore, the matrix to be decomposed has its size reduced d times, being used d times in solution steps.

Furthermore, the procedure shown for $\boldsymbol{\Pi_l^0 \varepsilon}$ in [23] requires the decomposition of a $(3n_l \times 3n_l)$ matrix $\boldsymbol{G}$ and a $(3n_l \times 2n_{DOF})$ matrix $\boldsymbol{B}$. However, one can assemble this projector matrix directly using the ones for the partial derivatives, as shown in (10).

Therefore, if one can compute Π_k^S, Π_k^0, and $\Pi_l^0 \partial_{x_j}$, for a given element, one can assemble the vector-solution counterparts for the first two ($\boldsymbol{\Pi_k^S}$, $\boldsymbol{\Pi_k^0}$), and compose the linear strain combination of the last ones ($\boldsymbol{\Pi_l^0 \varepsilon}$). The economy becomes even more drastic when one considers the three-dimensional case, as not only does the d-fold economy in the size of the decomposed matrix help, but the dimension of the polynomial space (n_l) increases more quickly with respect to the order l in higher spatial dimensions.

Additionally, in a more implementation minded way, it is easier to test and debug the projectors for a simpler formulation (Poisson's equations). Thus, one can implement element projectors based on Poisson's equations, validate them with patch tests and convergence studies, and then employ them to assemble more complex element formulations with the certainty of correct behavior on their part.

5 NUMERICAL EXAMPLES

Two convergence studies are presented to validate the proposed process. Both studies show the convergence of linear and quadratic virtual elements in both formulations for a problem with cubic solution. In the results, the serendipity formulation with stabilization is addressed as "SV" and the stabilization free one as "SFV". The second study shows the convergence of plane linear elasticity virtual elements whose projectors are assembled from the ones of the former study. For both problems the domain is the unit square centered on the origin. The same three polygonal meshes with different levels of refinement (represented by maximum element diameter h) are used in both examples. Those are illustrated in Figure 1.

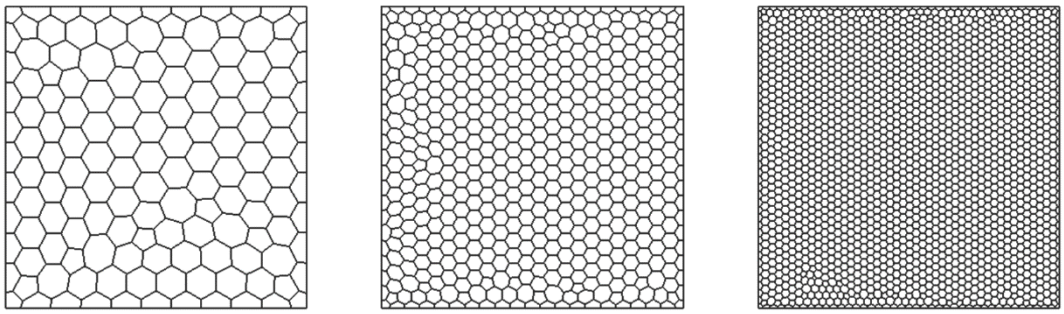

Figure 1: Polygonal meshes with different levels of refinement.

For each problem, two types of errors are computed: an L^2-error for the solution, and an error based on the derivates (H^1-error for Poisson problem and $\boldsymbol{\varepsilon}$-error for elasticity). The relationship between mesh refinement (h) and error (e) is of the following form

$$e = Ch^p, \tag{11}$$

with the exponent p being $k+1$ for L^2-type errors and k for the derivative based errors in the case of optimal *a priori* estimates.

5.1 Poisson Convergence Study

This study consists in a Poisson problem designed around a 3rd order polynomial solution, so that both linear and quadratic elements can have their convergence rates assessed. The chosen solution is the one in (12) and illustrated in Figure 2. The problem was setup as a pure Dirichlet problem (i.e., prescribed values at the boundary).

$$u = 3(x^3 + y^3 + xy) \tag{12}$$

Three meshes with Voronoi polygons were generated with different levels of refinement, and the both the L^2-(13) and H^1-(14) errors are computed using the L^2 projections of the solution and the gradient.

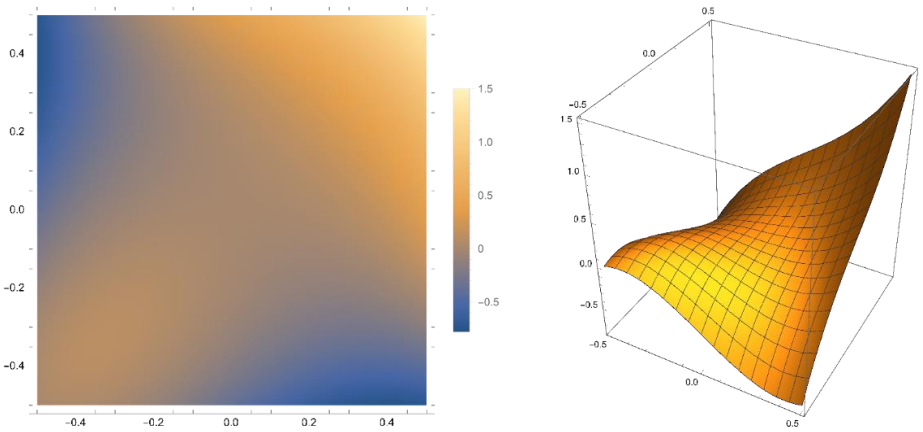

Figure 2: Solution chosen for the Poisson convergence study.

$$\|e\|_{L^2} = \sqrt{\sum_E \int_E (u - \Pi_k^0 u_h)^2 d\boldsymbol{x}} \tag{13}$$

$$|e|_{H^1} = \sqrt{\sum_E \int_E (\nabla u - \Pi_l^0 \nabla u_h)^2 d\boldsymbol{x}} \tag{14}$$

The results are summarized in Table 1 and visually in Figure 3.

Table 1: Error results from Poisson convergence study.

	L^2-error			p	H^1-error			p
Mesh	M1	M2	M3		M1	M2	M3	
h	1.33E-01	6.81E-02	3.33E-02		1.33E-01	6.81E-02	3.33E-02	
SVO1	3.63E-03	1.04E-03	2.66E-04	1.88	2.00E-01	1.08E-01	5.50E-02	0.93
SFVO1	3.60E-03	1.03E-03	2.63E-04	1.89	1.28E-01	6.89E-02	3.49E-02	0.93
SVO2	1.13E-04	1.52E-05	1.91E-06	2.94	8.29E-03	2.19E-03	5.54E-04	1.95
SFVO2	1.12E-04	1.51E-05	1.91E-06	2.93	7.96E-03	2.07E-03	5.20E-04	1.97

The convergence rates p found in Table 1 are in accordance with the *a priori* estimates for these elements, found in the beginning of the section.

5.2 Elasticity Convergence Study

For this example, a simple solution displacement field is chosen, as presented in (15) and illustrated in Figure 4. The problem setup chosen for the attainment for this solution is illustrated in Figure 5. The L^2 (16) and $\boldsymbol{\varepsilon}$ (17) errors are computed using the respective analog projections. The stabilization employed for the serendipity formulation is the one presented in [23]. A summary of the results is presented in Table 2 and Figure 6.

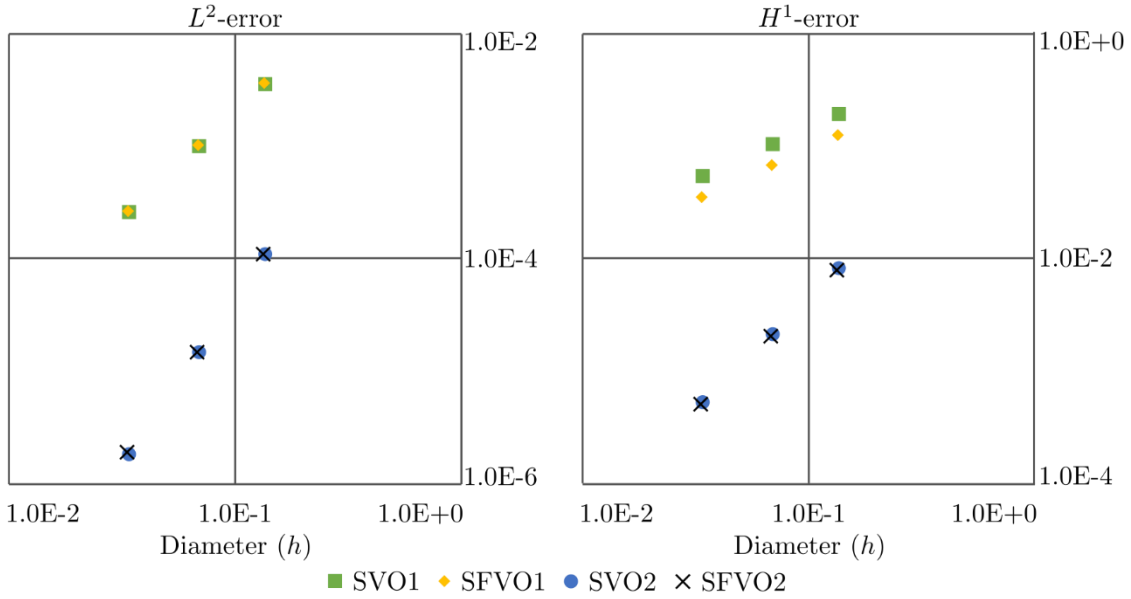

Figure 3: Convergence curves of L^2-error (left) and H^1-error (right) for the Poisson study.

$$\boldsymbol{u} = \{(x + 0.5)/6 \quad 0\}^T \tag{15}$$

$$\|\boldsymbol{e}\|_{L^2} = \sqrt{\sum_E \int_E \left(\boldsymbol{u} - \boldsymbol{\Pi}_k^0 \boldsymbol{u}_h\right)^2 d\boldsymbol{x}} \tag{16}$$

$$|\boldsymbol{e}|_{\boldsymbol{\varepsilon}} = \sqrt{\sum_E \int_E \left(\boldsymbol{\varepsilon}(\boldsymbol{u}) - \boldsymbol{\Pi}_l^0 \boldsymbol{\varepsilon}(\boldsymbol{u}_h)\right)^2 d\boldsymbol{x}} \tag{17}$$

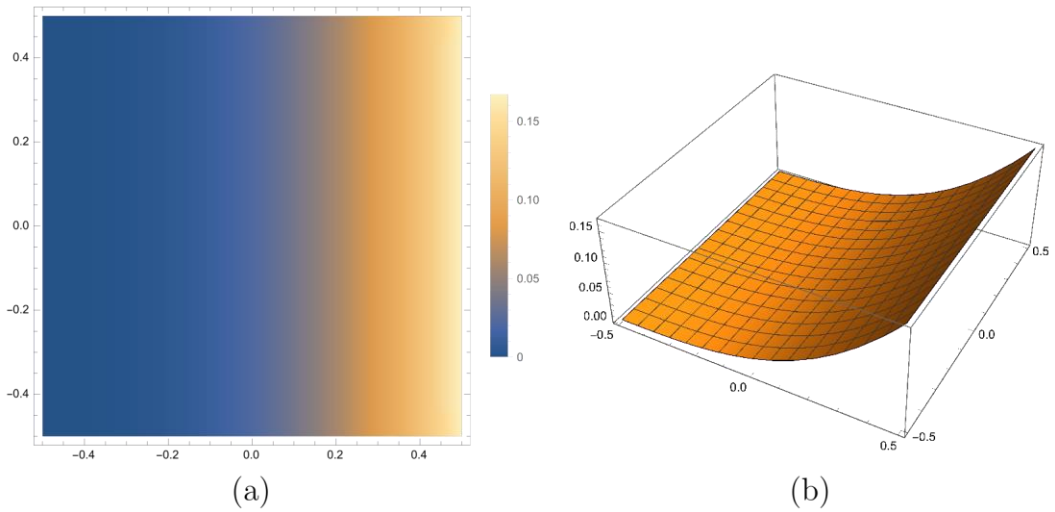

Figure 4: Solution chosen for the elasticity convergence study.

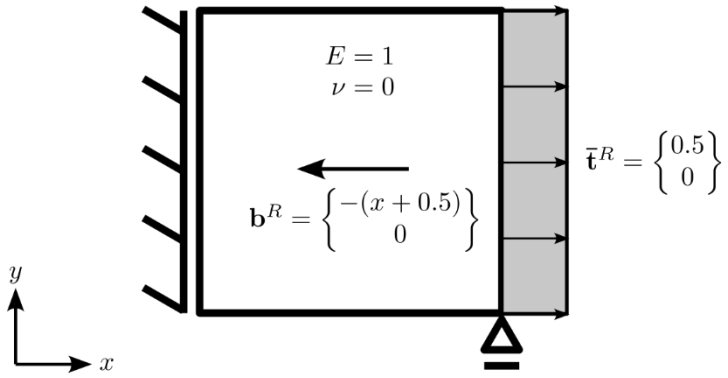

Figure 5: Problem setup for elasticity convergence study.

Table 2: Error results from elasticity convergence study.

Mesh	L^2-error			p	$\boldsymbol{\varepsilon}$-error			p
	M1	M2	M3		M1	M2	M3	
h	1.33E-01	6.81E-02	3.33E-02		1.33E-01	6.81E-02	3.33E-02	
SVO1	3.18E-04	8.20E-05	2.06E-05	1.97	1.44E-02	7.45E-03	3.76E-03	0.97
SFVO1	3.27E-04	8.41E-05	2.14E-05	1.96	1.06E-02	5.42E-03	2.73E-03	0.98
SVO2	8.02E-06	6.92E-07	1.16E-07	3.05	3.42E-04	9.01E-05	2.22E-05	1.97
SFVO2	5.34E-06	6.97E-07	8.47E-08	2.99	3.04E-04	8.33E-05	2.09E-05	1.93

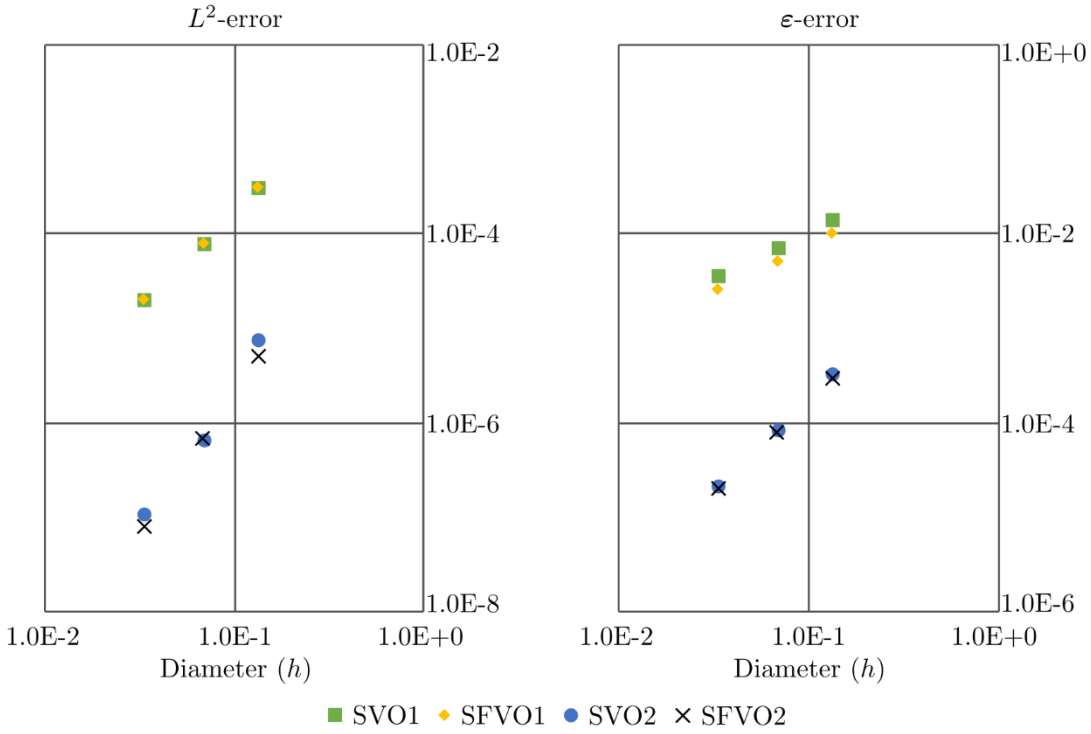

Figure 6: Convergence curves of L^2-error (left) and $\boldsymbol{\varepsilon}$-error (right) for the elasticity study.

One can see that the optimal convergence rates are preserved by the projector assembly process.

6 FINAL CONSIDERATIONS

The procedure of assembling complex projectors from simpler ones has been presented. It is a small matter which may help slightly improve the computational efficiency of VEM codes by reducing the size of matrices that have to be decomposed to obtain the projectors.

This framework to constructing virtual element implementations also provides Poisson's equations as simpler context in which to test and debug the necessary projectors.

The provided examples show that this procedure preserves the convergence of the method.

REFERENCES

[1] L. Beirão da Veiga, F. Brezzi, A. Cangiani, G. Manzini, L. D. Marini, and A. Russo, "Basic Principles of Virtual Element Methods," *Mathematical Models and Methods in Applied Sciences*, vol. 23, no. 01, pp. 199–214, 2013, doi: 10.1142/S0218202512500492.

[2] B. Ahmad, A. Alsaedi, F. Brezzi, L. D. Marini, and A. Russo, "Equivalent projectors for virtual element methods," *Computers and Mathematics with Applications*, vol. 66, no. 3, pp. 376–391, 2013, doi: 10.1016/j.camwa.2013.05.015.

[3] L. Beirão da Veiga, F. Brezzi, L. D. Marini, and A. Russo, "Serendipity Nodal VEM spaces," *Comput Fluids*, vol. 141, pp. 2–12, 2016, doi: 10.1016/j.compfluid.2016.02.015.

[4] F. Brezzi, R. S. Falk, and L. D. Marini, "Basic principles of mixed Virtual Element Methods," *ESAIM: Mathematical Modelling and Numerical Analysis*, vol. 48, no. 4, pp. 1227–1240, 2014, doi: 10.1051/m2an/2013138.

[5] A. Cangiani, G. Manzini, and O. J. Sutton, "Conforming and nonconforming virtual element methods for elliptic problems," *IMA Journal of Numerical Analysis*, vol. 37, no. 3, p. drw036, Aug. 2016, doi: 10.1093/imanum/drw036.

[6] L. Beirão da Veiga and G. Manzini, "A virtual element method with arbitrary regularity," *IMA Journal of Numerical Analysis*, vol. 34, no. 2, pp. 759–781, 2014, doi: 10.1093/imanum/drt018.

[7] H. Chi, A. Pereira, I. F. M. Menezes, and G. H. Paulino, "Virtual element method (VEM)-based topology optimization: an integrated framework," *Structural and Multidisciplinary Optimization*, vol. 62, no. 3, pp. 1089–1114, Sep. 2020, doi: 10.1007/s00158-019-02268-w.

[8] P. F. Antonietti, M. Bruggi, S. Scacchi, and M. Verani, "On the virtual element method for topology optimization on polygonal meshes: A numerical study," *Computers and Mathematics with Applications*, vol. 74, no. 5, pp. 1091–1109, 2017, doi: 10.1016/j.camwa.2017.05.025.

[9] C. Böhm, L. Munk, B. Hudobivnik, F. Aldakheel, J. Korelc, and P. Wriggers, "Virtual Elements for computational anisotropic crystal plasticity," *Comput Methods Appl Mech Eng*, vol. 405, p. 115835, Feb. 2023, doi: 10.1016/j.cma.2022.115835.

[10] M. Pingaro, M. L. De Bellis, E. Reccia, P. Trovalusci, and T. Sadowski, "Fast Statistical Homogenization Procedure for estimation of effective properties of Ceramic Matrix Composites (CMC) with random microstructure," *Compos Struct*, vol. 304, p. 116265, Jan. 2023, doi: 10.1016/j.compstruct.2022.116265.

[11] M. Pingaro, E. Reccia, P. Trovalusci, and R. Masiani, "Fast statistical homogenization procedure (FSHP) for particle random composites using virtual element method," *Comput Mech*, vol. 64, no. 1, pp. 197–210, Jul. 2019, doi: 10.1007/s00466-018-1665-7.

[12] M. Marino, B. Hudobivnik, and P. Wriggers, "Computational homogenization of polycrystalline materials with the Virtual Element Method," *Comput Methods Appl Mech Eng*, vol. 355, pp. 349–372, Oct. 2019, doi: 10.1016/j.cma.2019.06.004.

[13] A. Gay Neto, B. Hudobivnik, T. F. Moherdaui, and P. Wriggers, "Flexible polyhedra modeled by the virtual element method in a discrete element context," *Comput Methods Appl Mech Eng*, vol. 387, Dec. 2021, doi: 10.1016/j.cma.2021.114163.

[14] M. Cihan, B. Hudobivnik, J. Korelc, and P. Wriggers, "A virtual element method for 3D contact problems with non-conforming meshes," *Comput Methods Appl Mech Eng*, 2022, doi: 10.1016/j.cma.2022.115385.

[15] P. Wriggers and W. T. Rust, "A virtual element method for frictional contact including large deformations," *Eng Comput (Swansea)*, vol. 36, no. 7, pp. 2133–2161, Aug. 2019, doi: 10.1108/EC-02-2019-0043.

[16] A. Chen and N. Sukumar, "Stabilization-free serendipity virtual element method for plane elasticity," *Comput Methods Appl Mech Eng*, vol. 404, p. 115784, Feb. 2023, doi: 10.1016/j.cma.2022.115784.

[17] L. Beirão Da Veiga, F. Brezzi, F. Dassi, L. D. Marini, and A. Russo, "Serendipity Virtual Elements for General Elliptic Equations in Three Dimensions," *Chinese Annals of Mathematics. Series B*, vol. 39, no. 2, pp. 315–334, 2018, doi: 10.1007/s11401-018-1066-4.

[18] B.-B. Xu and P. Wriggers, "3D stabilization-free virtual element method for linear elastic analysis," *Comput Methods Appl Mech Eng*, vol. 421, p. 116826, Mar. 2024, doi: 10.1016/j.cma.2024.116826.

[19] L. Beirão Da Veiga, F. Brezzi, L. D. Marini, and A. Russo, "Virtual Element Method for general second-order elliptic problems on polygonal meshes," *Mathematical Models and Methods in Applied Sciences*, vol. 26, no. 4, pp. 729–750, 2016, doi: 10.1142/S0218202516500160.

[20] A. M. D'Altri, S. de Miranda, L. Patruno, and E. Sacco, "An enhanced VEM formulation for plane elasticity," *Comput Methods Appl Mech Eng*, vol. 376, p. 113663, Apr. 2021, doi: 10.1016/j.cma.2020.113663.

[21] B.-B. Xu, F. Peng, and P. Wriggers, "Stabilization-free virtual element method for finite strain applications," *Comput Methods Appl Mech Eng*, vol. 417, p. 116555, Dec. 2023, doi: 10.1016/j.cma.2023.116555.

[22] L. Beirão da Veiga, F. Brezzi, L. D. Marini, and A. Russo, "The Hitchhiker's Guide to the Virtual Element Method," *Mathematical Models and Methods in Applied Sciences*, vol. 24, no. 08, pp. 1541–1573, 2014, doi: 10.1142/S021820251440003X.

[23] E. Artioli, L. Beirão da Veiga, C. Lovadina, and E. Sacco, "Arbitrary order 2D virtual elements for polygonal meshes: part I, elastic problem," *Comput Mech*, vol. 60, no. 3, pp. 355–377, Sep. 2017, doi: 10.1007/s00466-017-1404-5.